β-delayed fission of ^{230}Am

G. L. Wilson,[1,2] M. Takeyama,[3,4] A. N. Andreyev,[1,5,6] B. Andel,[7] S. Antalic,[7] W. N. Catford,[8] L. Ghys,[9,10] H. Haba,[3] F. P. Heßberger,[11,12] M. Huang,[3] D. Kaji,[3] Z. Kalaninova,[7,13] K. Morimoto,[3] K. Morita,[3,14] M. Murakami,[3,15] K. Nishio,[5] R. Orlandi,[5] A. G. Smith,[16] K. Tanaka,[3,17] Y. Wakabayashi,[3] and S. Yamaki[3,18]

[1]*Department of Physics, University of York, York, YO10 5DD, United Kingdom*
[2]*Department of Physics and Applied Physics, University of Massachusetts Lowell, Lowell, Massachusetts 01854, USA*
[3]*Nishina Center for Accelerator-Based Science, RIKEN, Wako, Saitama 351-0198, Japan*
[4]*Department of Physics, Yamagata University, Yamagata 990-8560, Japan*
[5]*Advanced Science Research Center, Japan Atomic Energy Agency, Tokai, Ibaraki 319-1195, Japan*
[6]*ISOLDE, CERN, Geneva CH-1211, Switzerland*
[7]*Department of Nuclear Physics and Biophysics, Comenius University in Bratislava, 84248 Bratislava, Slovakia*
[8]*Department of Physics, University of Surrey, Guildford, Surrey, GU2 7XH, United Kingdom*
[9]*Instituut voor Kern- en Stralingsfysica, University of Leuven, Celestijnenlaan 200 D, B-3001 Leuven, Belgium*
[10]*Belgian Nuclear Research Center SCK•CEN, Boeretang 200, B-2400 Mol, Belgium*
[11]*Gesellschaft fur Schwerionenforschung Darmstadt, Postfach 110541, 6100 Darmstadt, Germany*
[12]*Helmholtz Institut Mainz, 5099 Mainz, Germany*
[13]*Laboratory of Nuclear Problems, JINR, 141980 Dubna, Russia*
[14]*Department of Physics, Kyusyu University, Motooka, Fukuoka 819-0395, Japan*
[15]*Department of Chemistry, Niigata University, Niigata 950-2181, Japan*
[16]*School of Physics and Astronomy, University of Manchester, Manchester, M13 9PL, United Kingdom*
[17]*Faculty of Science and Technology, Tokyo University of Science, Noda, Chiba 278-8510, Japan*
[18]*Department of Physics, Saitama University, Saitama 338-8570, Japan*

(Received 19 February 2017; revised manuscript received 7 September 2017; published 13 October 2017)

The exotic decay process of β-delayed fission (βDF) has been studied in the neutron-deficient isotope ^{230}Am. The ^{230}Am nuclei were produced in the complete fusion reaction ^{207}Pb(^{27}Al,4n)^{230}Am and separated by using the GARIS gas-filled recoil ion separator. A lower limit for the βDF probability $P_{\beta\mathrm{DF}}(^{230}\mathrm{Am}) > 0.30$ was deduced, which so far is the highest value among all known βDF nuclei. The systematics of βDF in the region of ^{230}Am will be discussed.

DOI: 10.1103/PhysRevC.96.044315

I. INTRODUCTION

β-delayed fission (βDF) is a rare two-step nuclear-decay process in which the parent nuclide first undergoes β decay (β^+/EC or β^-) populating excited states in the daughter nucleus. If the excitation energy E^* of the populated states is comparable to, or even higher than, the fission barrier height B_f of the daughter nuclide, then fission may happen instantaneously in competition with γ and/or particle emission. The observed half-life behavior of fission events in βDF is determined by the half-life of the feeding β-decaying parent nucleus. Up to now, 28 βDF nuclides are known, all of them being odd-odd; see the references in the recent review [1] and the study of ^{240}Es and ^{236}Bk in [2]. An important experimental quantity is the βDF probability, which is defined as the ratio of the number of βDF decays, $N_{\beta\mathrm{DF}}$, to the number of β decays, N_β, of the parent nuclide:

$$P_{\beta\mathrm{DF}} = \frac{N_{\beta\mathrm{DF}}}{N_\beta}. \quad (1)$$

β-delayed fission was discovered in the neutron-deficient isotopes ^{232,234}Am in Dubna in 1966 [3]. These nuclides were further studied in more detail in follow-up experiments in Dubna [4], Berkeley [5,6], and Karlsruhe [7]. Though different experimental techniques and analysis assumptions were used by Kuznetsov *et al.* [4] (Dubna, 1967) and Hall *et al.* [6,8] (Berkeley, 1990) in their respective studies of ^{234}Am, very comparable values of $P_{\beta\mathrm{DF}}(^{234}\mathrm{Am})$ were deduced, see Table I.

The isotope ^{232}Am was studied in three experiments, which reported three very different $P_{\beta\mathrm{DF}}$ values, see Table I. The groups from Dubna [3] and Berkeley [5] used the same experimental techniques and assumptions as for their respective studies of ^{234}Am. However, the Dubna group reported a $P_{\beta\mathrm{DF}}(^{232}\mathrm{Am})$ value which is 100 times larger than that deduced by the Berkeley group. Furthermore, the Dubna result is ∼5 times higher than a measurement undertaken by Habs *et al.* in Karlsruhe in 1978 [7]. The reason for such a large difference between three measurements of $P_{\beta\mathrm{DF}}(^{232}\mathrm{Am})$ is as yet unknown. It should be noted that the value obtained by the Berkeley group [5], being the lowest of the three, is thought to be the most accurate; see discussion in [1]. However, for the consistency of the discussion, all three values of $P_{\beta\mathrm{DF}}(^{232}\mathrm{Am})$ have been plotted in Fig. 1, which shows the measured $P_{\beta\mathrm{DF}}$ values as a function of the Q_{EC}(parent)$-B_f$(daughter) difference. Here, 13 nuclides with "reliably measured" $P_{\beta\mathrm{DF}}$ values, as evaluated by Ref. [1], were used, with an addition

TABLE I. Calculated Q_{EC} values for electron capture and fission barrier heights, B_f, for βDF of ^{230,232,234}Am (from Refs. [9] and [10], respectively). Literature $P_{\beta DF}$ values for ^{232,234}Am and our experimental lower limit for ^{230}Am are given in the last column.

EC/β^+ decay	Parent Q_{EC} (MeV) [9]	Daughter B_f (MeV) [10]	$Q_{EC} - B_f$ (MeV)	EC/β^+ branch (%)	$T_{1/2}$ (precursor) (min)	$P_{\beta DF}$
^{234}Am → ^{234}Pu	4.12	3.83	0.29	∼100 [6]	2.32(8) [6]	∼6.95×10^{-5}, Dubna [4] $6.6(18) \times 10^{-5}$, Berkeley [6]
^{232}Am → ^{232}Pu	4.88	3.23	1.65	∼97 [5]	1.31(4) [5]	6.96×10^{-2}, Dubna [3] $(1.3^{+4}_{-0.8}) \times 10^{-2}$, Karlsruhe [7] $6.9(10) \times 10^{-4}$, Berkeley [5]
^{230}Am → ^{230}Pu	5.68	3.07	2.61	∼100	0.52, this work[a]	>0.30, this work

[a]The weighted average of measurements from this work and GARIS [11], see text.

of two recently reported values for ^{240}Es and ^{236}Bk from [2]. Figure 1 shows an overall linear dependence of $\log(P_{\beta DF})$ on the Q_{EC}(parent) − B_f(daughter) difference. However, a caveat should be mentioned here that the plots of logarithmic $P_{\beta DF}$ values (and the partial βDF half-life values $T_{1/2,\beta DF}$, which can be obtained from $P_{\beta DF}$, see [12]) can show somewhat different, but still linear, trends if one uses different models to estimate Q_{EC} and B_f values; see the discussion of Fig. 12 in [1] or Fig. 4 of [12].

The very neutron-deficient isotope ^{230}Am is expected to possess one of the largest differences of Q_{EC}(parent) − B_f(daughter) ∼ 2.61 MeV for βDF nuclides; see Table I and Fig. 1. By using the $P_{\beta DF}$ for ^{232}Am obtained in Berkeley and extrapolating $P_{\beta DF}(^{232,234}\text{Am})$ data to ^{230}Am in Fig. 1, a value of $P_{\beta DF}(^{230}\text{Am}) \sim 10^{-2}$ (∼1%) can be estimated. However, in the case of using the much higher values of $P_{\beta DF}(^{232}\text{Am})$ from Karlsruhe or Dubna, a much higher extrapolated probability of $P_{\beta DF}(^{230}\text{Am})$ would be obtained, approaching 100%. Therefore, a measurement of $P_{\beta DF}(^{230}\text{Am})$ would allow a better insight into the systematics of βDF in this region of extremely neutron-deficient nuclei.

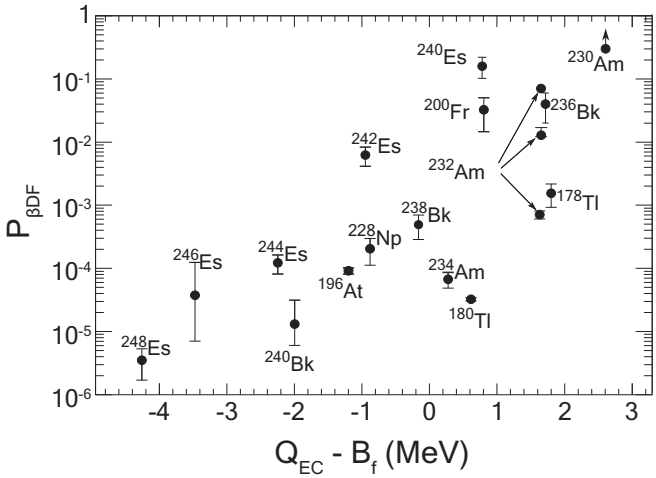

FIG. 1. Experimental $P_{\beta DF}$ values as a function of the Q_{EC}(parent) − B_f(daughter) difference. Calculated Q_{EC} and B_f values are taken from Refs. [9,10], using the finite-range droplet model (FRDM) and the finite-range liquid drop model (FRLDM), respectively. Three values of $P_{\beta DF}$ for ^{232}Am are presented (see Table I); the value of $P_{\beta DF}$ for ^{230}Am is from this work.

In an earlier experiment at RIKEN's gas-filled recoil ion separator (GARIS) (coupled to the gas-jet system), aimed at the identification of the new isotope ^{234}Bk in the reaction ^{197}Au(^{40}Ar,3n)^{234}Bk, six fission events following α decays of ^{234}Bk were reported, and a suggestion was made that these fission events could be due to the βDF of ^{230}Am [11]. We note that no α decay of ^{230}Am was observed in the GARIS study, which allows a first experimental determination of the β-decay branch of ^{230}Am as $b_\beta(^{230}\text{Am}) > 90\%$. This estimate is in agreement with a value of $b_\beta(^{230}\text{Am}) \sim 75\%$, which was calculated using a predicted partial β-decay half-life of 42.3 s from Möller *et al.* [13] and the total half-life of $T_{1/2}(^{230}\text{Am}) = 32^{+22}_{-9}$ s, determined from six fission events in Ref. [11]. A particular limitation of this work with respect to fission measurements was that due to the experimental method used, no fission fragment energies could actually be measured, and only "high energy" saturated signals were registered for events above 20 MeV; see details in Ref. [11].

Therefore, we decided to undertake a dedicated experiment to study possible βDF of ^{230}Am by directly producing this isotope in the complete fusion reaction ^{207}Pb(^{27}Al,4n)^{230}Am. Due to the direct production (rather than via the α decay of ^{234}Bk) a higher production cross section could be expected.

II. EXPERIMENTAL SETUP

In the present experiment, a beam of 145-MeV ^{27}Al ions was delivered by the RIKEN heavy ion linear accelerator (RILAC). The beam was provided at an intensity of 0.5–1.5 pμA (where 1 pμA = 6.24×10^{12} particles/s) for 6 days. Three modes of beam pulsing were used, with the "beam-ON/beam-OFF" intervals of 40 s/40 s, 5 s/5 s and 20 s/60 s. These modes represent 20%, 31%, and 49% of the data collection periods, respectively.

The rotating ^{207}Pb target was installed in the gas-filled target chamber of GARIS with the helium gas at a pressure of 0.5 mbar. The use of a differential pumping system in front of the target chamber avoided the need of an extra window to separate the high vacuum of the beam-transport system and the helium-gas-filled separator. This allowed the use of the higher beam intensities and to reduce the ^{27}Al beam scattering. Sixteen ^{207}Pb target segments were mounted onto a rotating-wheel target frame. The thickness of the targets ranged from 340 to 430 μg/cm^2, the carbon target backing had a thickness of 60 μg/cm^2. The target wheel rotated at 3600 rpm.

The reaction products of interest recoiling out of the target (hereafter called "recoils") were separated by GARIS from

the primary beam and unwanted background products such as scattered target recoils and transfer reaction products. GARIS consists of four magnets in $D1$-$Q1$-$Q2$-$D2$ configuration (further details provided in Ref. [14]), with $B\rho$ set to 1.8 Tm in this work. The detection chamber, situated at the focal plane of GARIS at a distance of 6.16 m from the target, was separated from the gas-filled volume of GARIS by a 0.5-μm-thick Mylar foil and evacuated down to 10^{-6} mbar.

For the measurements in the 40/40 s and 5/5 s beam-ON/beam-OFF modes, the separated recoils passed two time-of-flight (TOF) detectors, each consisting of a 0.5-μm-thick Mylar foil with an effective area of 78 mm in diameter. Signals were obtained from secondary electrons which are emitted when ions pass through the foils and are collected by microchannel plates. After passing these TOF detectors, recoils were implanted into a position-sensitive silicon detector (PSD), with a total area of 58×58 mm^2 divided into 16 longitudinal strips. Upstream of the PSD, four unsegmented silicon detectors, also with an active area of 58×58 mm^2, were mounted in a "box" configuration. These detectors, hereafter called "BOX detectors," were used to measure the energies of α particles and fission fragments escaping from the PSD in the backward direction. The signals from the TOF detectors were used to distinguish decay events in the PSD and the implantation events by requiring an anticoincidence condition between the signals from the PSD and from at least one of the TOF detectors. The same PSD-BOX detection system was exploited in the measurements with the 20/60 s beam pulsing mode, but no TOF detectors were used. The combined PSD-BOX detection efficiency for α particles was $\epsilon_\alpha = 85\%$, and for double-fold coincident fission fragments, $\epsilon_{\rm FF} = 70\%$ [14].

The energy calibration of the PSD and the BOX detectors in the region of fission fragments with energies of up to ~150 MeV (see below) relied on the extrapolation of the calibration based on α decays of ^{211}At and ^{211}Po isotopes [with energy 5869.5(22) and 7450.3(5) keV, respectively [15]], produced in the same reaction after a few-nucleon transfer on the ^{207}Pb target. The energy of the initial ^{27}Al beam leaking through GARIS with low intensity was also used as a calibration point, after accounting for the energy losses in the target, TOF, and other foils. This procedure does not account for the pulse-height defect for fission fragments being measured by the silicon PSD and BOX detectors; this issue will be discussed further in the text. A typical energy resolution for α particles measured only by PSD varied between the strips in the range of 34 to 105 keV (FWHM) at 7450 keV.

III. EXPERIMENTAL RESULTS

A. β-delayed fission of ^{230}Am

Figure 2(a) shows the total energy spectrum of all events registered in the PSD in the reaction ^{207}Pb(^{27}Al,4n)^{230}Am at the beam energy of $E(^{27}\text{Al}) = 145$ MeV in front of the target. A few groups of events can be distinguished in the spectrum. The highest energy group corresponds to the "full" energy ^{27}Al beam projectiles "leaking" through GARIS with low intensity. The broad structure around and below ~30 MeV corresponds to the scattered target-like nuclei and target-like

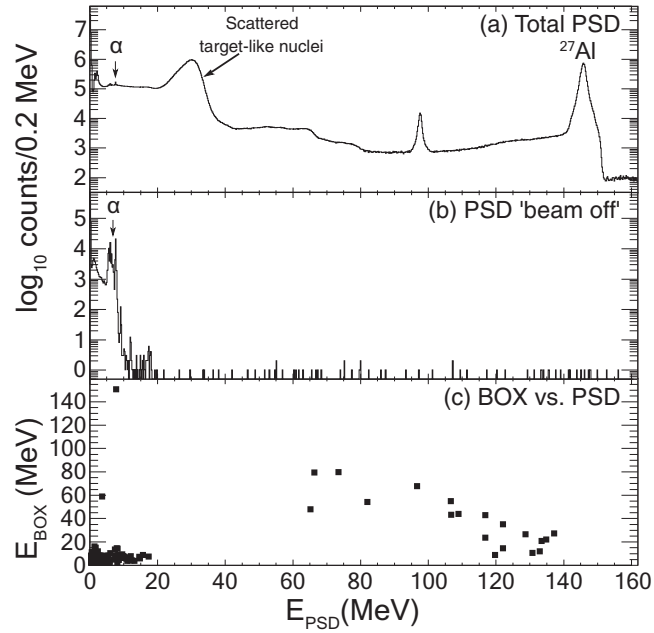

FIG. 2. (a) Total energy spectrum in the PSD in the reaction ^{207}Pb(^{27}Al,4n)^{230}Am. The peaks are described in the text. (b) The same as (a), but within the beam-OFF interval (either 40, 5, or 60 s, see text), and with a TOF anticoincidence condition when the TOF detectors were used. (c) Two-dimensional BOX vs PSD spectrum, with the same gating conditions as (b). A threshold condition, that $E_{\rm BOX} > 2$ MeV and $E_{\rm PSD} > 2$ MeV, has been applied.

transfer products. The broadly distributed structure with the energy in the range of 40–140 MeV is due to lower energy scattered ^{27}Al ions. The α decays of the implanted recoil nuclei and their daughters are seen at $E_{\rm PSD} < 9$ MeV. The reason for the low-intensity peak at ~95 MeV is not clear, most probably it could be some beam contaminant with a similar A/q ratio as that of the ^{27}Al beam.

Figure 2(b) shows the same spectrum as Fig. 2(a), but registered only during the beam-OFF time intervals, which corresponds to either 40, 5, or 60 s, depending on the mode of beam pulsing used. An extra 5 ms is excluded from the start of the beam-OFF interval, to further suppress beam and beam-like products to be registered in the PSD after the beam is switched off. An anticoincidence condition between the signals from the PSD and from at least one of the TOF detectors was additionally required for the data collected in the 40 and 5 s beam-OFF modes, when the TOF detectors were still exploited. Therefore only decay events should be present in this spectrum. Indeed, the beam and recoil/transfer product peaks disappear, but a number of counts above 20 MeV are still present.

Here we note that we are aware of a small contamination of the GARIS target chamber with the ^{248}Cm target material, used in some of the previous long-running experiments aimed at the production of superheavy elements. ^{248}Cm is a long-lived ($T_{1/2} = 3.5 \times 10^5$ yr) isotope with a spontaneous fission branching ratio of $b_{\rm SF} = 8.39\%$. The total kinetic energy release for fission fragments is TKE(^{248}Cm) = 182.2 MeV, with the most probable energies for light and heavy mass

peaks of 103.4 and 78.7 MeV, respectively [16]. The fission fragments from ^{248}Cm can pass through GARIS with some probability and be registered in the PSD as *single-fold* events, producing some of the high-energy events in the region above 20 MeV and up to ∼100 MeV in Fig. 2(b). To quantify this, two dedicated background measurements were performed with no beam on the target. In the first measurement, the valve between the target chamber and GARIS was closed, thus no fission fragments from ^{248}Cm could reach the PSD. In this mode, within 215 h of measurements, a single double-fold event with energy of $E_{\mathrm{PSD}} = 18$ MeV, $E_{\mathrm{BOX}} = 43$ MeV was observed. In the second measurement, the valve between the target chamber and GARIS was open, allowing ^{248}Cm fission fragments to pass through GARIS and to be registered in the PSD. In this mode, within 55 h of measurements, 81 single events in the energy range of $E_{\mathrm{PSD}} = 20$–100 MeV were observed, with no events above 100 MeV. Based on the above data, we can conclude that the region of 20–100 MeV in Fig. 2(b) can contain the fission events from both spontaneous fission of ^{248}Cm and from βDF of ^{230}Am (see below). In contrast to this, no events from ^{248}Cm should be present above 100 MeV in Fig. 2(b), where only the events from βDF of ^{230}Am and from any remaining leaked ^{27}Al can occur.

Despite the presence of the aforementioned background, the unique distinction between the *single-fold* background fission events due to ^{248}Cm (also the leaked ^{27}Al beam) and the βDF of ^{230}Am can be done via the detection of prompt *double-fold* PSD-BOX events with large energy deposition (see below). This method provides an unambiguous selection of fission fragments, emitted back-to-back in the βDF of ^{230}Am nuclei implanted in the PSD. The two-dimensional E_{BOX}-E_{PSD} spectrum corresponding to events in Fig. 2(b) is shown in Fig. 2(c). An energy condition of $E_{\mathrm{BOX}} > 2$ MeV and $E_{\mathrm{PSD}} > 2$ MeV was applied to eliminate random coincidences with low-energy background events and electronics and/or detector noise. A total of 19 double-fold fission events with $E_{\mathrm{PSD}} > 50$ MeV were detected, which, as shown in Sec. III B, should be attributed to the βDF of ^{230}Am.

An estimate of the total kinetic energy release, TKE(^{230}Pu), could be done by summing the measured PSD+BOX energies for these 19 fission events. In such a way, an "apparent" TKE(^{230}Pu) ∼ 146 MeV was obtained. However, the detector calibration procedure used (based on α particles and ^{27}Al beam) does not account for the pulse-height defect of fission fragments in the silicon detectors and their energy loss in the dead layers. As shown in the previous work at the separator for heavy ion reaction products (SHIP) velocity filter at GSI (Ref. [17], for example), this effect can be as high as 20–50 MeV and depends on the implantation depth [18,19]. In the present study a similar calibration procedure was used, based on the measurements of the apparent TKE values for the fission fragments from the spontaneous fission of ^{252}No (produced in a separate experiment at GARIS) as a function of the implantation depth and comparing them to the tabulated TKE value [20]. A respective energy correction of 24(14) MeV was deduced in our study, which, after summing up with the apparent TKE value mentioned above, resulted in the full value of TKE(^{230}Pu) = 170(20) MeV. This value is ∼10 MeV lower than the expected value of TKE=180 MeV following the Viola systematics [21], but it is still in agreement within a rather large uncertainty of our measurement.

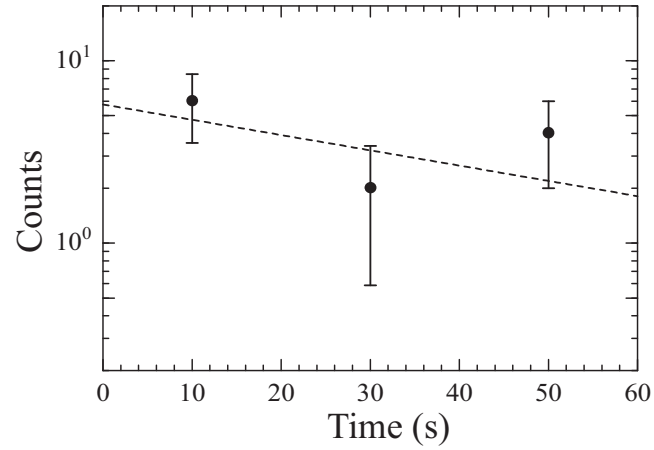

FIG. 3. Time distribution of 12 double-fold fission events collected in the 60 s beam-OFF time interval of the 20/60 s beam pulsing mode measurements, with an exponential fit shown by a dashed line.

To deduce the half-life of ^{230}Am, the data from the 20/60s beam-ON/beam-OFF measurements were used. Figure 3 shows the time distribution of 12 double-fold fission events observed within the 60 s beam-OFF interval, together with a fit with an exponential function. The resulting half-life $T_{1/2}(^{230}\mathrm{Am}) = 36^{+15}_{-8}$ s agrees with a value of $T_{1/2} = 32^{+22}_{-9}$ s deduced in Ref. [11], based on six observed fission events. By combining the data from both experiments, a value of $T_{1/2}(^{230}\mathrm{Am}) = 36^{+12}_{-7}$ s was deduced.

A production cross section of ∼540 pb was deduced for the production of ^{230}Am in the reaction channel ^{207}Pb(^{27}Al,4n)^{230}Am at the beam energy used in this study. A calculated GARIS transmission efficiency of 20% was used to derive this value.

B. Assignment of fission events to βDF of ^{230}Am

First we will discuss the assignment of the 19 observed fission events to β-delayed fission of ^{230}Am rather than to its spontaneous fission (SF) decay. This was done based on systematics of SF half-lives and hindrance factors, as described, for example, in the reviews by Hoffman *et al.* [22] and by Heßberger [23] and references therein. As shown in Fig. 17 in Ref. [23], spontaneous fission in odd-A nuclides is typically hindered by a large factor of 10^3–10^5 relative to their even-even neighbours. This hindrance is believed to originate due to the so-called specialization energy [24] arising from the spin/parity conservation for the odd nucleon in the fission process. It is furthermore expected that the SF hindrance factors for the odd-odd nuclides can be approximately estimated to be the product of the hindrance factors for the odd-neutron and odd-proton neighbors. Indeed, as reviewed in Refs. [22,23], hindrance factors in excess of 10^6 were reported for a number of spontaneously fissioning odd-odd isotopes in the transuranium region.

A qualitative estimate for the expected SF half-life of ^{230}Am could be done in the following way: the closest even-even

nuclide with a known SF decay is ^{234}Cm [23,25] which has a half-life of 51(12) s, comparable to that of ^{230}Am. The evaluated partial SF half-life is ~1500 s [23,25]. By applying a hindrance factor of 10^6, a partial SF half-life of ~10^9 s would be deduced for ^{230}Am, which in turn would result in a negligible SF branch, based on the comparison to the measured half-life of ^{230}Am.

To further confirm our assignment, we mention that none of the lower-Z elements, which could be potentially produced in any evaporation channel (pxn or αxn) of the reaction used or in any transfer channel on the lead target, has a SF decay with a half-life comparable to our experimental value. Furthermore, the only possible candidate for βDF with lower-Z value, i.e., ^{228}Np, has a $P_{\beta\mathrm{DF}} = 2.0(9) \times 10^{-4}$ [26], which combined with its strongly reduced production in the $\alpha 2n$ channel (see next section) excludes this isotope from being the source of the observed βDF activity in our study. Finally, the fact that the same activity seems to be produced in a different reaction in the earlier experiment at GARIS [11] adds another confirmation of the correctness of our identification.

C. Evaluation of $P_{\beta\mathrm{DF}}(^{230}\mathrm{Am})$

In our work, the $P_{\beta\mathrm{DF}}(^{230}\mathrm{Am})$ was deduced from the data collected in the 60 s beam-OFF interval in the 20/60s beam pulsing mode. By definition [see Eq. (1)], the βDF probability for ^{230}Am can be calculated from

$$P_{\beta\mathrm{DF}}(^{230}\mathrm{Am}) = \frac{N_{\beta\mathrm{DF}}(^{230}\mathrm{Am})}{N_{\beta}(^{230}\mathrm{Am})}, \tag{2}$$

where $N_{\beta\mathrm{DF}}(^{230}\mathrm{Am}) = 12$ is the number of observed double-fold fission events and $N_{\beta}(^{230}\mathrm{Am})$ is the number of β decays of ^{230}Am which occurred in this mode.

The number of β decays of ^{230}Am cannot be measured directly in our experiment, but by definition it is equal to the sum of the number of βDF events of ^{230}Am, $N_{\beta\mathrm{DF}}(^{230}\mathrm{Am})$, and the number of the daughter ^{230}Pu nuclei, $N(^{230}\mathrm{Pu})$, see Eq. (3)(a), after proper corrections for respective detection efficiencies and branching ratios, where needed

$$\begin{aligned} N_{\beta}(^{230}\mathrm{Am}) &= \frac{N_{\beta\mathrm{DF}}(^{230}\mathrm{Am})}{\epsilon_{\mathrm{FF}}} + N(^{230}\mathrm{Pu}), && (a)\\ &= \frac{N_{\beta\mathrm{DF}}(^{230}\mathrm{Am})}{\epsilon_{\mathrm{FF}}} + \frac{N_{\alpha}(^{230}\mathrm{Pu})}{b_{\alpha}(^{230}\mathrm{Pu})}, && (b)\\ &= \frac{N_{\beta\mathrm{DF}}(^{230}\mathrm{Am})}{\epsilon_{\mathrm{FF}}} + \frac{N_{\alpha\alpha}(^{230}\mathrm{Pu} - {}^{226}\mathrm{U})}{b_{\alpha}(^{230}\mathrm{Pu}) \times \epsilon_{\alpha}^2 \times 0.94}. && (c) \end{aligned} \tag{3}$$

The $N(^{230}\mathrm{Pu})$ value is deduced from the number of observed α decays of ^{230}Pu, $N_{\alpha}(^{230}\mathrm{Pu})$, corrected, as shown in Eq. (3)(b), for the α-decay branching ratio $b_{\alpha}(^{230}\mathrm{Pu})$. An upper limit for the latter was experimentally and model-independently deduced as $b_{\alpha}(^{230}\mathrm{Pu}) > 73\%$ in Ref. [25], it will be further used to calculate the value of $P_{\beta\mathrm{DF}}(^{230}\mathrm{Am})$. In passing we note that a comparable value of $b_{\alpha}(^{230}\mathrm{Pu}) = 84\%$ was evaluated in [27] by using the calculated β-decay half-life (no uncertainty was given in the original paper).

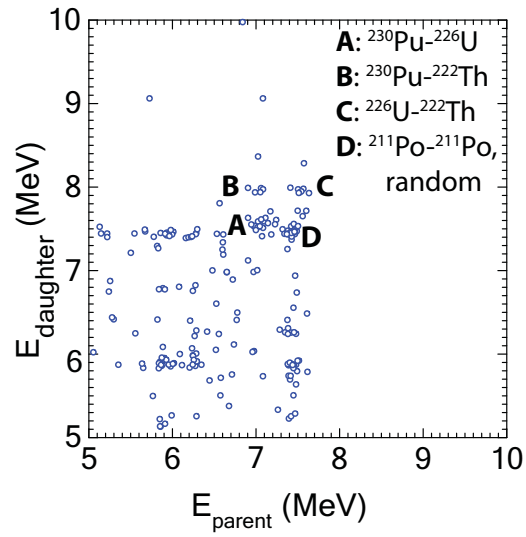

FIG. 4. α-α correlation plot, created for the time interval $\Delta T(\alpha\text{-}\alpha) \leqslant 1$ s and position window of $\Delta X(\alpha\text{-}\alpha) \leqslant 2$ mm. The groups originating from the decay of ^{230}Pu are labeled with symbols A, B, C. Group D represents the random self-correlations between the 7.45 MeV α decays of ^{211}Po, abundantly produced in a transfer reaction channel on the ^{207}Pb target.

In our work, the number $N_{\alpha}(^{230}\mathrm{Pu})$ was determined by searching for time-position correlated α decays of ^{230}Pu with the energy of 7.06 MeV with the known α decays of its daughter isotope ^{226}U [$T_{1/2} = 260(10)$ ms], similar to studies [25,27,28]. By exploiting both PSD and BOX detectors (thus also adding up the PSD+BOX signals for the "escaping" particles), $N_{\alpha\alpha}(^{230}\mathrm{Pu}\text{-}^{226}\mathrm{U}) = 22$ correlation chains were observed, marked as group A in Fig. 4. This value was then used in Eq. (3)(c). The applied energy window for α decay of ^{226}U included both the g.s.→ g.s. [7.560 MeV, 86(3)%] and g.s.→ 2^+ (^{222}Th) [7.384 MeV, 14(3)%] α-decay branches, thus no additional correction was needed. The factor of 0.94 in Eq. (3)(c) accounts for the fact that only the correlation interval of four half-lives was used for Fig. 4. The factor of ϵ_{α}^2 accounts for the efficiency of measuring a two-member α-α correlation chain $^{230}\mathrm{Pu} \rightarrow {}^{226}\mathrm{U}$. We note that we also observed further correlations to granddaughter ^{222}Th ($E_{\alpha} = 7.98$ MeV, $T_{1/2} = 2.24$ ms); see, e.g., the groups B and C in Fig. 4. The correlations with the follow-up decays of ^{218}Ra and ^{214}Rn were also registered, often leading to higher-energy pile-up events, due to the very short half-lives of these isotopes (25.6 and 0.27 μs, respectively); see, e.g., Fig. 1 of [28]. These events are not shown in Fig. 4 solely for the sake of the simplicity of this figure.

Finally, by combining Eqs. (2) and (3)(c), the $P_{\beta\mathrm{DF}}(^{230}\mathrm{Am})$ can be calculated as shown in Eq. (4).

$$P_{\beta\mathrm{DF}}(^{230}\mathrm{Am}) = \frac{N_{\beta\mathrm{DF}}(^{230}\mathrm{Am})/\epsilon_{\mathrm{FF}}}{\frac{N_{\beta\mathrm{DF}}(^{230}\mathrm{Am})}{\epsilon_{\mathrm{FF}}} + \frac{N_{\alpha\alpha}(^{230}\mathrm{Pu}-{}^{226}\mathrm{U})}{b_{\alpha}\times\epsilon_{\alpha}^2\times 0.94}}. \tag{4}$$

The application of Eq. (4) relies on the assumption that the direct production of ^{230}Pu via the $p3n$ evaporation channel of the $^{27}\mathrm{Al} + {}^{207}\mathrm{Pb}$ reaction is about a factor of 10 lower than the

production of ^{230}Am, which was estimated by using statistical model code HIVAP [29]. Therefore, most of the α-decay chains of ^{230}Pu observed in the data should have originated after ^{230}Pu was produced via the EC/β^+ decay of ^{230}Am. Due to this, the $N_{\alpha\alpha}(^{230}\mathrm{Pu} - ^{226}\mathrm{U})$ number was reduced by 10% due to the possible direct production of ^{230}Pu in the reaction rather than after β decay of ^{230}Am. Finally, a *lower* limit of $P_{\beta\mathrm{DF}}(^{230}\mathrm{Am}) > 0.30$ was deduced by using Eq. (4).

We note that no correlated α-decay chains of the type $^{230}\mathrm{Am} \rightarrow ^{226}\mathrm{Np}$ were observed, which establishes that the β-decay branch of ^{230}Am is indeed close to 100% (shown in Table I), in agreement with the estimates given in Sec. I.

Based on HIVAP calculations, we also estimated that the production cross section in the αxn channel is lower by a factor of 5 relative to the xn channel. Due to a broader angular distribution of products in the αxn channel, it will be further suppressed by the entrance aperture of GARIS, in comparison to the xn and pxn channels.

IV. DISCUSSION

The deduced $P_{\beta\mathrm{DF}}(^{230}\mathrm{Am})$ value is the highest so far among all "reliably" measured βDF probabilities, as defined in Ref. [1]; see also Fig. 1. With the present measurement, the chain of americium isotopes ^{230,232,234}Am becomes the third one for which more than two isotopes with the measured $P_{\beta\mathrm{DF}}$ values are known, the other chains being that of five einsteinium nuclides ^{240,242,244,246,248}Es and of three berkelium isotopes ^{236,238,240}Bk. This figure also demonstrates that while the three $P_{\beta\mathrm{DF}}$ values for ^{230,232,234}Am follow the overall increasing trend [as a function of the Q_{EC}(parent) $-$ B_f(daughter) difference] of other nuclides, the ^{230}Am value is somewhat higher with respect to the linear extrapolation (from a semilogarithmic plot) from ^{232,234}Am values. However, as mentioned in Sec. I, a value of $P_{\beta\mathrm{DF}}(^{230}\mathrm{Am}) \sim 0.01$ would be extrapolated if one uses the Berkeley data for ^{232}Am, while much higher values would result if either Dubna or Karlsruhe data were used. This discrepancy for ^{230}Am may imply that the Berkeley value for ^{232}Am could be underestimated, while the measurements by Dubna or Karlsruhe groups could be more accurate.

It is also interesting to note in Fig. 1 the difference in the overall trends of the $P_{\beta\mathrm{DF}}$ values for the chain of the Es and Bk isotopes on the one hand and the Am isotopes on the other hand. Indeed, one notices a similar slope for the Es and Bk values. In contrast to this, the Am isotopes demonstrate a very different slope, irrespective of which value is taken for ^{232}Am. A possible reason for this difference could be the fact that most data points for the Es and Bk isotopes have negative $Q_{\mathrm{EC}} - B_f$ values, leading to predominantly subbarrier fission. The latter is mostly determined by the barrier penetrability, thus is expected to have a linear dependence on the $Q_{\mathrm{EC}} - B_f$ difference, while the β-strength function is expected to play a less important role. In the case of the Am isotopes, all three measured data points have positive $Q_{\mathrm{EC}} - B_f$ values (at least in the mass model used for Fig. 1), which opens up the possibility of above-barrier fission, which does not need to follow the linear trend. In this case, also the role of β-strength function might become more important. These considerations show the importance of studying βDF of even lighter isotopes, ^{228}Am, ^{234}Bk, and ^{238}Es, all of which should have large positive $Q_{\mathrm{EC}} - B_f$ differences and large $P_{\beta\mathrm{DF}}$ probabilities.

Due to the lack of detailed nuclear spectroscopy information on the decay of ^{230}Am, a discussion of the possible structure of ^{230}Am, e.g., spin, parity, and underlying configuration, would be highly tentative at this moment. As a general recommendation, dedicated β-decay studies of the lightest americium isotopes, e.g., by the mass-separator technique used in Refs. [30,31], should be performed. Such studies have been recently initiated at the mass separator coupled to the tandem at the Japan Atomic Energy Agency in Tokai, Japan [32].

V. CONCLUSIONS

The exotic process of β-delayed fission has been studied in the extremely neutron-deficient isotope ^{230}Am, produced directly in the complete fusion reaction $^{207}\mathrm{Pb}(^{27}\mathrm{Al}, 4n)^{230}\mathrm{Am}$. A lower limit for the value of the βDF probability $P_{\beta\mathrm{DF}}(^{230}\mathrm{Am}) > 0.30$ was deduced, which is the highest so far among all known nuclei. The experiment showed the prospects of extending such measurements to an even more neutron-deficient isotope ^{228}Am, in which a value close to 100% would be expected, based on an even larger Q_{EC}(parent) $-$ B_f(daughter) $= 3.73$ MeV difference in comparison to ^{230}Am.

ACKNOWLEDGMENTS

This experiment was performed at the RI Beam Factory operated by RIKEN Nishina Center and CNS, the University of Tokyo. This work has been funded by FWO-Vlaanderen (Belgium), by the Slovak Research and Development Agency (Contract No. APVV-0105-10 and No. APVV-14-0524) and the Slovak Grant Agency VEGA (Contract No. 1/0532/17), by the UK Science and Technology Facilities Council (STFC), and by the Reimei Foundation of JAEA.

[1] A. N. Andreyev, M. Huyse, and P. Van Duppen, Rev. Mod. Phys. **85**, 1541 (2013).

[2] J. Konki, J. Khuyagbaatar, J. Uusitalo, P. Greenlees, K. Auranen, H. Badran, M. Block, R. Briselet, D. Cox, M. Dasgupta, A. D. Nitto, C. Düllmann, T. Grahn, K. Hauschild, A. Herzán, R.-D. Herzberg, F. Heßberger, D. Hinde, R. Julin, S. Juutinen, E. Jäger, B. Kindler, J. Krier, M. Leino, B. Lommel, A. Lopez-Martens, D. Luong, M. Mallaburn, K. Nishio, J. Pakarinen, P. Papadakis, J. Partanen, P. Peura, P. Rahkila, K. Rezynkina, P. Ruotsalainen, M. Sandzelius, J. Sarén, C. Scholey, J. Sorri, S. Stolze, B. Sulignano, C. Theisen, A. Ward, A. Yakushev, and V. Yakusheva, Phys. Lett. B **764**, 265 (2017).

[3] V. I. Kuznetsov, N. K. Skobelev, and G. N. Flerov, Sov. J. Nucl. Phys. **4**, 202 (1967).

[4] V. I. Kuznetsov, N. K. Skobelev, and G. N. Flerov, Yad. Fiz. **5**, 271 (1967) [Sov. J. Nucl. Phys. **5**, 191 (1967)].
[5] H. L. Hall, K. E. Gregorich, R. A. Henderson, C. M. Gannett, R. B. Chadwick, J. D. Leyba, K. R. Czerwinski, B. Kadkhodayan, S. A. Kreek, N. J. Hannink, D. M. Lee, M. J. Nurmia, D. C. Hoffman, C. E. A. Palmer, and P. A. Baisden, Phys. Rev. C **42**, 1480 (1990).
[6] H. L. Hall, K. E. Gregorich, R. A. Henderson, C. M. Gannett, R. B. Chadwick, J. D. Leyba, K. R. Czerwinski, B. Kadkhodayan, S. A. Kreek, D. M. Lee, M. J. Nurmia, D. C. Hoffman, C. E. A. Palmer, and P. A. Baisden, Phys. Rev. C **41**, 618 (1990).
[7] D. Habs, H. Klewe-Nebenius, V. Metag, B. Neumann, and H. J. Specht, Z. Phys. A **285**, 53 (1978).
[8] H. L. Hall, K. E. Gregorich, R. A. Henderson, C. M. Gannett, R. B. Chadwick, J. D. Leyba, K. R. Czerwinski, B. Kadkhodayan, S. A. Kreek, D. M. Lee, M. J. Nurmia, and D. C. Hoffman, Phys. Rev. Lett. **63**, 2548 (1989).
[9] P. Möller, A. J. Sierk, T. Ichikawa, A. Iwamoto, R. Bengtsson, H. Uhrenholt, S. Åberg, Phys. Rev. C **79**, 064304 (2009).
[10] P. Möller, A. J. Sierk, T. Ichikawa, A. Iwamoto, and M. Mumpower, Phys. Rev. C **91**, 024310 (2015).
[11] D. Kaji, K. Morimoto, H. Haba, E. Ideguchi, H. Koura, and K. Morita, J. Phys. Soc. Jpn. **85**, 015002 (2016).
[12] L. Ghys, A. N. Andreyev, S. Antalic, M. Huyse, and P. Van Duppen, Phys. Rev. C **91**, 044314 (2015).
[13] P. Möller, J. Nix, and K.-L. Kratz, Atom. Data Nucl. Data **66**, 131 (1997).
[14] K. Morita, K. Morimoto, D. Kaji, H. Haba, E. Ideguchi, R. Kanungo, K. Katori, H. Koura, H. Kudo, T. Ohnishi, A. Ozawa, T. Suda, K. Sueki, I. Tanihata, H. Xu, A. V. Yeremin, A. Yoneda, A. Yoshida, Y.-L. Zhao, and T. Zheng, Eur. Phys. J. A **21**, 257 (2004).
[15] F. G. Kondev and S. Lalkovski, Nucl. Data Sheets **112**, 707 (2011).
[16] V. Kalinin, V. Dushin, F.-J. Hambsch, V. Jakovlev, K. Il'ya, A. Laptev, B. Petrov, G. Petrov, Y. Pleva, O. Shcherbakov, V. Sokolov, and A. Vorobyev, J. Nucl. Sci. Technol. **39**, 250 (2002).
[17] A. N. Andreyev, S. Antalic, D. Ackermann, L. Bianco, S. Franchoo, S. Heinz, F. P. Heßberger, S. Hofmann, M. Huyse, Z. Kalaninová, I. Kojouharov, B. Kindler, B. Lommel, R. Mann, K. Nishio, R. D. Page, J. J. Ressler, B. Streicher, S. Saro, B. Sulignano, and P. Van Duppen, Phys. Rev. C **87**, 014317 (2013).
[18] S. Hofmann, D. Ackermann, S. Antalic, H. G. Burkhard, V. F. Comas, R. Dressler, Z. Gan, S. Heinz, J. A. Heredia, F. P. Heßberger, J. Khuyagbaatar, B. Kindler, I. Kojouharov, P. Kuusiniemi, M. Leino, B. Lommel, R. Mann, G. Münzenberg, K. Nishio, A. G. Popeko, S. Saro, H. J. Schött, B. Streicher, B. Sulignano, J. Uusitalo, M. Venhart, and A. V. Yeremin, Eur. Phys. J. A **32**, 251 (2007).
[19] K. Nishio, S. Hofmann, F. P. Heßberger, D. Ackermann, S. Antalic, V. Comas, Z. Gan, S. Heinz, J. A. Heredia, H. Ikezoe, J. Khuyagbaatar, B. Kindler, I. Kojouharov, P. Kuusiniemi, B. Lommel, M. Mazzocco, S. Mitsuoka, Y. Nagame, T. Ohtsuki, A. G. Popeko, S. Saro, H. J. Schött, B. Sulignano, A. Svirikhin, K. Tsukada, K. Tsuruta, and A. V. Yeremin, AIP Conf. Proc. **891**, 71 (2007).
[20] M. Takeyama, D. Kaji, K. Morimoto, Y. Wakabayashi, F. Tokanai, and K. Morita, JPS Conf. Proc. **11**, 030004 (2016).
[21] V. E. Viola, K. Kwiatkowski, and M. Walker, Phys. Rev. C **31**, 1550 (1985).
[22] D. C. Hoffman, Nucl. Phys. A **502**, 21 (1989).
[23] F. P. Heßberger, Eur. Phys. J. A **53**, 75 (2017).
[24] P. Möller, J. Nix, and W. Swiatecki, Nucl. Phys. A **492**, 349 (1989).
[25] P. Cagarda *et al.*, in *Proceedings of the 5th International Conference "Dynamical Aspects of Nuclear Fission" (DANF)* (World Scientific, Singapore, 2002), p. 398.
[26] S. A. Kreek, H. L. Hall, K. E. Gregorich, R. A. Henderson, J. D. Leyba, K. R. Czerwinski, B. Kadkhodayan, M. P. Neu, C. D. Kacher, T. M. Hamilton, M. R. Lane, E. R. Sylwester, A. Türler, D. M. Lee, M. J. Nurmia, and D. C. Hoffman, Phys. Rev. C **50**, 2288 (1994).
[27] P. Greenlees, P. Kuusiniemi, N. Amzal, A. N. Andreyev, P. A. Butler, K. Cann, J. Cocks, O. Dorvaux, T. Enqvist, P. Fallon, B. Gall, M. Guttormsen, D. Hawcroft, K. Helariutta, F. P. Heßberger, F. Hoellinger, G. Jones, P. Jones, R. Julin, S. Juutinen, H. Kankaanpää, H. Kettunen, M. Leino, S. Messelt, M. Muikku, S. Ødegård, R. Page, A. Savelius, A. Schiller, S. Siem, W. Trzaska, T. Tveter, and J. Uusitalo, Eur. Phys. J. A **6**, 269 (1999).
[28] A. N. Andreyev, D. D. Bogdanov, V. I. Chepigin, A. P. Kabachenko, S. Sharo, G. M. Ter-Akopian, A. V. Yeremin, and O. N. Malyshev, Z. Phys. A **337**, 231 (1990).
[29] W. Reisdorf, Z. Phys. A **300**, 227 (1981).
[30] M. Asai, M. Sakama, K. Tsukada, S. Ichikawa, H. Haba, I. Nishinaka, Y. Nagame, S. Goto, Y. Kojima, Y. Oura, H. Nakahara, M. Shibata, and K. Kawade, Eur. Phys. J. A **23**, 395 (2004).
[31] M. Sakama, M. Asai, K. Tsukada, S. Ichikawa, I. Nishinaka, Y. Nagame, H. Haba, S. Goto, M. Shibata, K. Kawade, Y. Kojima, Y. Oura, M. Ebihara, and H. Nakahara, Phys. Rev. C **69**, 014308 (2004).
[32] M. Asai *et al.* (private communication).